Petrography and geochemistry of the Middle Siwalik sandstones (tertiary) in understanding the provenance of sub-Himalayan sediments in the Lish River Valley, West Bengal, India

ABHIK KUNDU[1], ABDUL MATIN[2] and PATRICK G. ERIKSSON[3]

[1] Department of Geology, Asutosh College, 92, S. P. Mukherjee Road, Kolkata – 700026, India; kundu.abhik@gmail.com.

[2]Department of Geology, University of Calcutta, 35, Ballygunge Circular Road, Kolkata-700029, India; abdul.aindia@gmail.com.

[3]Department of Geology, University of Pretoria, Pretoria 0002, South Africa; 1940patrickeriksson@gmail.com.

Abstract

A petrography–geochemistry-based evaluation of the provenance of the sandstones of the Tertiary Middle Siwalik Subgroup in the Lish River Valley, West Bengal, is presented. The framework grains in the sandstones suggest mixing of sediments from spatially separated gneissic, quartzitic and phyllitic source rocks. Modal values of different framework minerals suggest that recycled sediments in an orogenic setting were deposited in the Middle Siwalik basin in the area. The major and trace element ratios suggest dominantly felsic input and mixing with subordinate basic material in an upper continental crustal setup. The major and trace element data also indicate that rocks of a passive margin setting acted as the source to the sediments. The present paper postulates that the Middle Siwalik sediments were derived from pre-Himalayan gneissic and metabasic rocks of an erstwhile passive margin setting and presently forming the Higher and Lesser Himalaya, respectively. basin.

Key words**:** Middle Siwalik; Darjeeling Himalaya; Sandstone petrography; Major element oxide; Provenance

1. INTRODUCTION

Petrography and geochemistry of clastic sedimentary rocks are important tools to understand the character of sediment provenance (Critelli *et al.* 2008; Luca Caracciolo *et al.* 2012; Perri *et al.* 2013). Petrography of sandstones is widely used to understand the lithological character of the source rocks (e.g., Crook 1974; Folk 1974; Blatt *et al.* 1980; Potter 1986; Pettijohn *et al.* 1987; Critelli *et al.* 1990; Weltje 2002; Basu 2003) and to infer their possible tectonic setting (e.g., Dickinson and Suczek 1979; Dickinson 1985, 1988; Dickinson *et al.* 1983; Asiedu *et al.* 2000). These studies mostly used the mineralogy, alteration, textural attributes and modal values of framework grains within investigated sedimentary rocks. Modal values are used to understand the tectonic settings of the source rocks for Himalayan sediments

(Critelli and Ingersoll 1994; Garzanti *et al*. 1996; Kundu *et al.* 2012). To understand the type of source rocks and also their tectonic setting, different authors (e.g., Schwab 1975; Bhatia 1983, 1985; McLennan *et al.* 1983; Taylor and McLennan 1985; Roser and Korsch 1988; Nesbitt and Young 1989; Condie *et al.* 1991; Cullers 1994; Armstrong-Altrin and Verma 2004; Nagarajan *et al.* 2007) have also used major oxide and trace element quantities and ratios of the clastic sedimentary rocks.

Petrographic and geochemical techniques for provenance analysis of the Siwalik rocks of different regions along the sub-Himalayan belt have been applied successfully. Petrography has been used as a tool for this purpose by Chaudhri (1971), Parkash *et al.* (1980), Critelli and Ingersoll (1994), Crittelli and Garzanti (1994), Garzanti *et al*. (1996) and Kundu *et al.* (2012), while geochemistry of the Siwalik sedimentary rocks has been used by others (DeCelles *et al.* 1998; Najman and Garzanti 2000; Ranjan and Banerjee 2009).

The present work is aimed at elucidating the provenance of the clastic sedimentary rocks of the Late-Miocene Middle Siwalik Subgroup in the Lish River valley of Darjeeling district of West Bengal, using both petrographic and chemical data generated from sandstone samples, for a more complete understanding of the source of these Siwalik sediments of West Bengal. Studies comparing quantitative data from both mineralogical and geochemical analytical methods on the same sample set are uncommon (Von Eynatten *et al.* 2003).

2. GEOLOGICAL SETTING

The major tectonic units of the Himalayan orogen from north to south are the South Tibet Detachment (STD), Main Central Thrust System (MCT-1 and MCT-2), the Ramgarh Thrust (RT), the Main Boundary Thrust (MBT) and the Main Frontal Thrust (MFT) (Valdiya 1980; Yin 2006; Mukul 2010) (Figs. 1a, b). The MCT-1 carries granulite facies paragneisses (Darjeeling/Kanchenjunga Gneiss) and the MCT-2 carries amphibolite facies metamorphites (Paro-Lingtse Gneiss) of the Greater Himalayan Sequence over the metamorphic rocks of the RT sheet; the RT separates the Upper Lesser Himalayan sequence from the Lower Lesser Himalayan sequence (Valdiya 1980; Bhattacharyya and Mitra 2009) and the MBT separates the Lesser and sub-Himalayan sequences (Gansser 1964; Yin 2006) (Figs. 1a, b). The southernmost and youngest fault, the MFT, separates the Mio-Pliocene Siwalik Group, on its hanging wall from the unconsolidated recent alluvium of the Indo-Gangetic plains in its footwall (Hodges 2000; Yin 2006 and references therein). In the Darjeeling and Jalpaiguri districts in eastern Himalaya, the MFT is not exposed and can only be recognized from scarps cutting the river terraces (Malik and Nakata 2003). In this area only the Lower and Middle

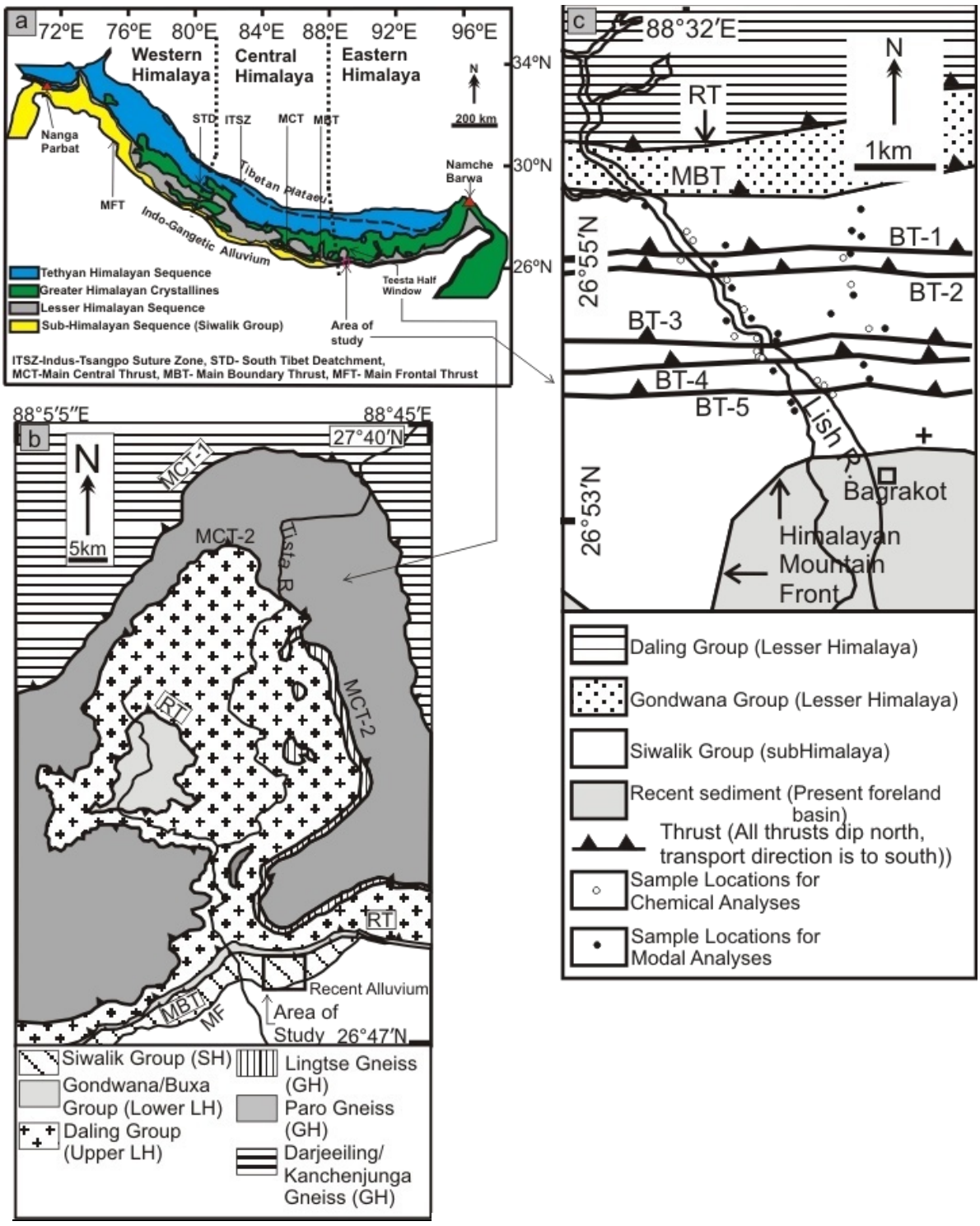

Figure 1. (a) Generalised Geological map of the Himalayan mountain belt (after Yin, 2006). The area of study is shown; (b) Generalised geological map of the Tista half-window in the Darjeeling-Sikkim Himalaya (simplified after Schwan 1980; Bhattacharyya and Mitra 2009). MCT-1: and MCT-2: Main Central Thrust (1 and 2), RT-Ramgarh Thrust, MBT-Main Boundary Thrust, MF-Mountain front. Area of present study is marked in rectangular box; (c) Geological map of the area of study. BT-1, BT-2, BT-3, BT-4 and BT-5 are thrusts punctuating the Middle Siwalik Group. RT-Ramgarh thrust, MBT-Main Boundary Thrust.

Table 1

Stratigraphy of the Darjeeling-Sikkim Himalaya (after Sinha Roy 1967; Acharyya and Shastry 1979; Acharyya 1994).

Age		Group	Subgroup		Lithology
Recent sediments of present day foreland basin					
----------MFT----------					
Cenozoic	Late Miocene – Pliocene	Siwalik Group	Upper Siwalik Subgroup	Murti Boulder bed	Crude immature conglomerate
				Parbu Grit	Pebbly sandstone and coarse-to-Medium sandstone
			Middle Siwalik Subgroup	Geabdat Sandstone	Medium to coarse-grained sandstone and shale, pebble beds and marl
	Early-Mid Miocene		Lower Siwalik Subgroup	Chunabati Formation	Fine to medium-grained sandstone, siltstone, mudstone, marl and conglomerate
----------MBT----------					
Palaeozoic	Upper Permian	Gondwana Group	Damuda Subgroup		Sandstone, carbonaceous shale and coal
	Lower Permian		Rangit Pebble-Slate		Diamictite, rythmite, quartzite and marl
----------RT----------					
Precambrian		Daling Group	Buxa Formation		Dolomites, quartzites and pyritiferous shales.
			Reyang Formation		Variegated quartzites, shales and slates.
					Chlorite–sericite, greenish phyllite, quartzite and slates, interbanded phyllite, quartzite and metabasic slates.
----------MCT 2----------					
		Paro Gneiss			Parametamorphites with migmatitic and foliated granitic gneiss
		Lingtse Gneiss			Biotite-granitic gneiss
----------MCT 1----------					
		Darjeeling Gneiss / Kanchenjunga Gneiss			Two mica migmatitic gneiss (Granulite grade), garnetiferous mica schist

Siwalik rocks are exposed (Banerji and Banerji 1982; Kundu *et al.* 2012) in the MFT sheet. The Middle Siwalik rocks are deformed by several north dipping imbricate thrusts (Mukul 2000 and references therein; Kundu *et al.* 2011, 2012). The present area of study is within the frontal-most part of the Tista Half Window (Fig. 1b). The studied sub-Himalayan sequence in the Lish River valley is made up of a succession of coarse-, medium- and fine-grained sandstone, siltstone, mudrock and conglomerate (Table 1) of Late-Miocene Middle Siwalik affinity (Banerji and Banerji 1982). The Middle Siwalik sequence of Tista Valley at ~3km to the west of the present area of study was deposited in an alluvial fan setting in the tectonically active foreland of the Himalayan orogen (Banerji and Banerji 1982; Kundu *et al*. 2012, refer to their figure 6). Lower and Upper Siwalik rocks are not observed in exposures in this area. The Middle Siwalik sequence is structurally disturbed by five north dipping thrust faults (addressed as BT-1, BT-2, BT-3, BT-4 and BT-5; from north to south, Fig. 1c). These faults are identified from the presence of slickensides, slickensides containing slickenlines, tens-of–cm-thick fault zones containing typical brittle fault rocks (cf. Sibson 1977; Blenkinsop 2002).

3. METHODS

The rocks were identified in the field and also in hand specimens following Pettijohn (1975) and Compton (1985). Sedimentary facies and facies associations have been identified on the basis of lithology and sedimentary structures (Selley, 1985) to explain the processes involved in the formation of the sequence of rocks (cf., Reading and Levell 1996; Neves *et al.* 2005). Considering the north dipping MFT that carries the Siwalik and also the north dipping thrusts (BT-1 to BT-5) that deform the sequence, the palaeocurrent data are rotated (cf. Ragan 2009) to bring them to original orientation. The resultant (pre-thrusting) palaeocurrent data are used to construct rose diagrams through the Georient 9.0 software (Holocombe 1994) to understand the palaeocurrent patterns. Twenty sandstone samples were studied under the petrographic microscope for understanding the mineralogy, textural attributes and signatures of deformation and alteration of the framework grains as well as the nature of the matrix (Pettijohn *et al.* 1987; Dorsey 1988; Garzanti and Vezzoli 2003). According to suggestions by Crook (1974), (Schwab 1975) and Dickinson and Suczek (1979) plate tectonics has a clear control on the modal compositions of sand and thereafter mineralogy of the framework grains of the sandstones became an established tool for inferring plate tectonic setting of the sources of sediments (Weltje and Von Eynatten 2004 and references therein). Counting of 300-350 points per thin section was done following the Gazzi-Dickinson point-counting method

(Gazzi 1966; Dickinson 1970; Ingersoll *et al.* 1984). Well-sorted medium-grained sandstones were considered for point counting in order to reduce the effect of grain-size (Lee and Sheen 1998). The counting grid used had apertures larger than the average size of framework grains in order to avoid repetition of counting on individual grains. Framework constituents were classified into monocrystalline quartz (Qm), polycrystalline quartz (Qp), (Qm + Qp = total quartz (Qt)), feldspar (F), sedimentary and metasedimentary lithic fragments (Ls) and volcanic lithic fragments (Lv), (Ls + Lv = (L)) according to the established schemes proposed by Dickinson and Suczek (1979), Dickinson *et al.* (1983) and Dickinson (1985). Results of point-counts recalculated to 100% are presented in Table 2. Modal values of total quartz (Q),

Table 2
Results of point-counts (recalculated to 100) on the framework grains from sandstone samples following Gazzi-Dickinson point-count method.

Samples	Qm	Qp	Q= (Qm+Qp)	F	Ls	Lv	L= (Lv+Ls)	Lt= (L+Qp)
WP14	60.3	3.46	63.76	16.6	19.64	0	19.64	23.1
WP11	57.98	8.56	66.54	9.63	23.83	0	23.83	32.39
WP08	60.36	10.5	70.86	10.46	18.68	0	18.68	29.18
C6A	64.24	5.46	69.7	16.35	13.95	0	13.95	19.41
C5	62.35	6.58	68.93	5.5	25.57	0	25.57	32.15
C2B	66.42	6.2	72.62	8.12	19.26	0	19.26	25.46
C2	60.68	8.1	68.78	12.28	18.94	0	18.94	27.04
B4	63.22	9.24	72.46	11.56	15.98	0	15.98	25.22
B31A	61.05	7.3	68.35	12.4	19.25	0	19.25	26.55
B26	60.24	9.32	69.56	8.2	22.24	0	22.24	31.56
B25A	58.85	13.94	72.79	13.68	13.53	0	13.53	27.47
B2	62.62	12.66	75.28	14.16	10.56	0	10.56	23.22
B17	66.54	12.44	78.98	16.54	4.48	0	4.48	16.92
B12	62.46	11.65	74.11	14.64	11.25	0	11.25	22.9
A9	60.1	9.86	69.96	13.8	16.24	0	16.24	26.1
A8A	63.27	6.45	69.72	14.25	16.03	0	16.03	22.48
A18	66.42	2.4	68.82	13.36	17.82	0	17.82	20.22
A16	65.44	5.2	70.64	14.26	15.1	0	15.1	20.3
A11	60.5	6.98	67.48	14.6	17.92	0	17.92	24.9
A1	63.8	5.8	69.6	14.1	16.3	0	16.3	22.1

feldspar (F) and lithic constituents (L) within the framework are also used to classify the sandstones (cf. Folk 1974). With only 20 sandstone samples analyzed by these methods, there would be little point in using histograms, statistical techniques or facies-based discrimination of sandstone modal values. However, all such sandstone petrographic data are in the end

proportions, and thus constrained by their constant-sum nature (i.e., all the variables concerned add up to a constant value, a total of 100% or, alternatively reflect values between 0 and 1) (cf., Aitchison 1986); as a result, the variables (mineralogy determined by point-counting) will not change independently of each other, resulting in the data not having a multivariate normal distribution and thus not allowing application of parametric statistical methods (Von Eynatten *et al.* 2003). Even in studies with much larger sample sets than the 20 examined here, petrographic-mineralogical studies are not well suited to multivariate discriminatory analysis (e.g., Ibekken and Schleyer 1991; Von Eynatten *et al.* 2003, for example, used 52 samples).

The content of major element oxides, trace elements and rare earth elements in the 16 sandstone samples were analyzed in the laboratory of the Wadia Institute of Himalayan Geology, Dehra Dun, India. Fine-grained sandstones were selected for analysis as finer siliciclastic rocks are more suitable than the coarser rocks for chemical analysis (McLennan *et al.* 1993). Major oxides and trace elements were quantified in an XRF Sequential Spectrometer (XRF-Siemens SRS-3000) while the rare earth elements were quantified in an ICP-MS (ELAN-DRC-E). Precision and accuracy were examined with international standard reference samples SDO-1, GSS-4, SO-1. Measuring error in XRF may be 2-5% while that in ICP-MS is <5% (Khanna *et al.* 2009). Procedures of assay are described in Rollinson (1993) and in Khanna *et al.* (2009). The REE data were normalised relative to the Chondrite values (Taylor and McLennan 1985). The analytical data are presented in Table 3 and are plotted in different established diagrams to classify the sandstones and to explicate the source rock types and their possible tectonic settings. Microsoft Excel and Minpet programs were used to plot the chemical data.

Analysis of the mineralogy of sandstone grains, the one main method used here, enable sthe differentiation of detrital and diagenetic components of the rock, as well as offering the opportunity to also study grain textures; neither are accomplished through the second main method adopted here, geochemistry (Von Eynatten *et al.* 2003). The petrographical-mineralogical method, however, is time-consuming and also has incipient errors in the point-counting technique upon which it is based (e.g., Dickinson 1970; Ingersoll *et al.* 1984). Geochemistry offers not just more precise compositional data sets, but also rapid achievement of large numerical data sets (e.g., Rollinson 1993).

Table 3

Geochemical analysis of sandstones of Middle Siwalik Subgroup

Sample	3 E	3 B	4 B	WP13	WP22	WP24	WP20	WP23	WP25	WP30	WP33	WP25/1	18FW	19HW	17HW	BK28
	Wt%	Wt%	Wt%	Wt%	Wt%	Wt%	Wt%	Wt%	Wt%	Wt%	Wt%	Wt%	Wt%	Wt%	Wt%	Wt%
Na_2O	2.03	1.93	1.19	0.33	1.24	1.57	0.83	0.54	1.19	1.77	1.52	1.51	1.12	1.77	1.28	1.5
MgO	0.86	1.04	2.51	2.91	1.94	1.58	0.52	1.85	2.09	1.22	1.15	1.16	1.08	1.32	1.12	0.9
Al_2O_3	8.82	10.27	17.47	20.8	12.43	14.46	6.99	18.81	15.88	12.39	12.07	11.9	11.43	12.86	12.27	14.33
SiO_2	82.28	78.72	67.21	55.44	70.24	70.12	87.54	64.21	63.65	71.47	73.99	75.9	74.01	73.94	76.41	72.88
P_2O_5	0.07	0.04	0.08	0.07	0.07	0.01	0.01	0.01	0.12	0.47	0.12	0.12	0.13	0.1	0.04	0.1
K_2O	1.88	2.26	2.77	4.54	2.61	2.96	1.42	3.93	3.03	2.1	2.46	2.15	2.15	3.06	2.52	3
CaO	0.66	0.54	0.89	0.5	1.92	0.49	0.09	0.31	2.52	1.06	0.34	0.47	0.29	0.36	0.18	0.59
TiO_2	0.31	0.29	0.63	0.82	0.38	0.46	0.25	0.75	0.69	0.92	0.48	0.49	0.44	0.4	0.39	0.55
MnO	0.05	0.03	0.06	0.1	0.05	0.03	0.02	0.07	0.07	0.21	0.09	0.08	0.1	0.03	0.03	0.03
Fe_2O_3	1.98	2.14	4.62	8.46	3.13	2.91	1.22	5.34	4.61	6.97	4.01	2.93	5.24	2.75	2.66	2.87
LOI	1.61	1.74	0.87	6.99	4.11	3.73	2.24	4.87	4.96	2.69	2.21	2.24	2.69	2.07	2.22	2.53
	ppm	ppm	ppm	ppm	ppm	ppm	ppm	ppm	ppm	ppm	ppm	ppm	ppm	ppm	ppm	ppm
La	23.3	20.8	51.5	54.1	30	27.9	18.6	61.8	53.6	181	66	81.9	69.4	30.8	26.1	62
Ce	47.4	41.8	104.9	112.5	60	56.5	38.2	131.1	110.6	367.5	135.2	165.6	141.7	60.7	52	102
Pr	4.8	4.2	9.7	9.8	6	5.7	3.9	11.7	10	36.7	12.4	15.3	13.3	6.2	5.3	13.3
Nd	19	16.3	40.1	40.7	23.7	22.9	15.7	49.2	40.6	140.9	49.3	60.1	53.3	24	20.9	60
Sm	3.96	3.33	7.77	8.06	4.83	4.64	3.14	9.52	8.16	29	10	11.95	10.5	4.84	4.24	10.2
Eu	0.69	0.66	1.4	1.58	0.88	0.92	0.62	1.76	1.48	3.3	1.38	1.43	1.41	0.95	0.89	1.35
Gd	2.89	2.5	5.85	6.28	3.66	3.61	2.33	7	6.33	22.2	7.86	9.33	8.14	3.85	3.3	7.81
Tb	0.48	0.42	0.96	1.08	0.61	0.6	0.39	1.08	1.05	3.6	1.32	1.54	1.27	0.64	0.55	1.2
Dy	2.59	2.25	4.94	5.8	3.17	3.15	2.18	5.45	5.53	19.1	7.39	8.14	6.36	3.56	2.99	5.78
Ho	0.53	0.45	0.94	1.18	0.6	0.6	0.45	1	1.05	3.6	1.43	1.57	1.15	0.67	0.59	0.98
Er	1.55	1.34	2.64	3.38	1.71	1.7	1.34	2.82	2.96	10.4	4.22	4.54	3.17	1.91	1.7	2.67
Tm	0.22	0.19	0.36	0.48	0.24	0.23	0.2	0.4	0.42	1.5	0.61	0.64	0.43	0.27	0.237	0.36
Yb	1.39	1.15	2.12	2.87	1.46	1.36	1.16	2.31	2.38	9.2	3.63	3.77	2.45	1.52	1.41	2.21
Lu	0.21	0.17	0.32	0.4	0.22	0.2	0.18	0.35	0.35	1.4	0.55	0.57	0.37	0.22	0.21	0.33
Ba	378	400	638	637	423	473	358	626	484	672	568	569	628	459	450	721
Cr	25	52	151	111	296	90	21	223	71	360	37	44	64	32	38	46
V	28	33	75	117	44	58	30	93	73	86	41	53	49	42	44	4
Sc	2	3.9	10.5	13.2	6	6.1	2	13.2	9.6	10.7	4	6.8	3.5	6.8	6.2	6.7
Ni	8	9	22	45	14	16	8	31	24	16	15	13	22	16	16	15
Cu	12	13	26	47	12	14	12	30	24	16	14	14	16	14	14	18
Zn	36	38	62	97	45	43	30	90	64	51	48	47	55	43	51	47
Ga	9	12	17	27	11	14	7	22	16	12	14	11	13	12	11	13

Pb	14	14	16	18	15	14	13	18	16	16	16	14	16	15	15	15
Th	12	10	18	20	10	12	8	22	19	50	28	33	26	12	11	27
Rb	94	108	122	280	123	138	59	241	139	94	115	95	109	150	115	146
U	1.2	1	2.9	7.7	1.3	1.2	1	2.7	1.9	5.9	2.7	2.1	3.1	1	1	1.5
Sr	37	33	89	53	78	55	28	52	66	55	45	49	40	46	41	65
Y	19	16	26	28	20	19	13	25	29	82	34	33	35	19	19	26
Zr	141	104	239	123	116	128	101	261	266	507	302	282	310	146	133	251
Nb	10	9	14	19	9	11	6	18	16	22	12	13	11	10	10	11
Y/Ni	2.375	1.7778	1.1818	0.6222	1.4286	1.1875	1.625	0.8065	1.2083	5.125	2.2667	2.5385	1.5909	1.1875	1.1875	1.7333
Cr/V	0.89286	1.5758	2.0133	0.9487	6.7273	1.5517	0.7	2.3978	0.9726	4.186	0.9024	0.8302	1.3061	0.7619	0.8636	11.5
La/Th	1.94167	2.08	2.8611	2.705	3	2.325	2.325	2.8091	2.8211	3.62	2.3571	2.4818	2.6692	2.5667	2.3727	2.2963
Th/Sc	6	2.5641	1.7143	1.5152	1.6667	1.9672	4	1.6667	1.9792	4.6729	7	4.8529	7.4286	1.7647	1.7742	4.0299
Zr/Sc	70.5	26.667	22.762	9.3182	19.333	20.984	50.5	19.773	27.708	47.383	75.5	41.471	88.571	21.471	21.452	37.463

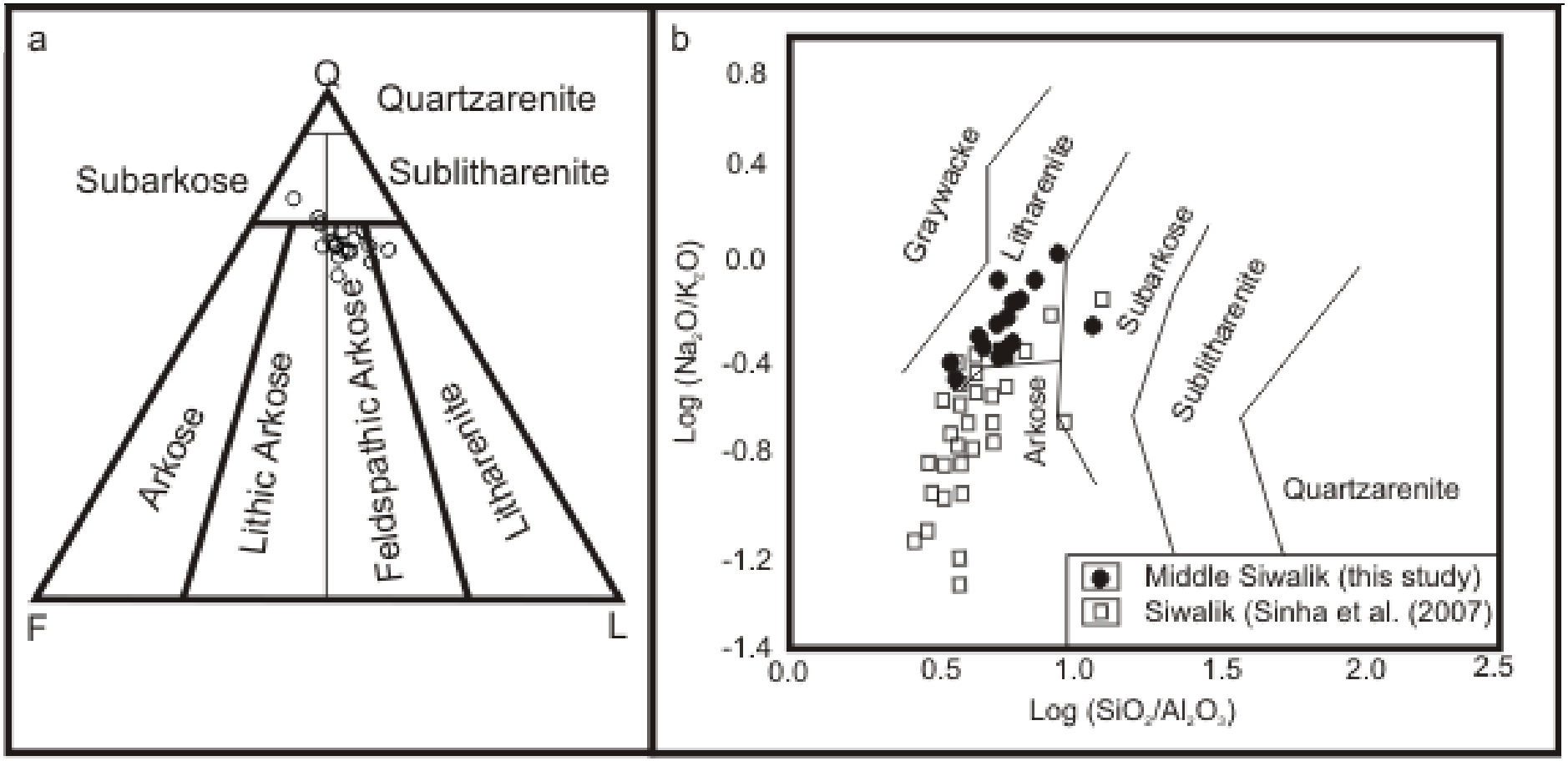

Figure 2. (a) Classification of Middle Siwalik sandstones of the Lish River valley after Folk (1974); (b) Chemical classification of Middle Siwalik sandstone samples in log (SiO2/Al2O3) *vs.* log (Na2O/K2O) diagram of Pettijohn *et al.* (1987). Shaded area encompasses plots of Lower and Middle Siwalik rocks from Punjab Recess by Sinha *et al.* (2007).

4. SANDSTONES TYPES

QFL values are plotted in the sandstone classification diagram of Folk (1974) where 14 samples fall in the feldspathic arkose field, 2 in the subarkose field, 1 in the lithic arkose field and 1 in the litharenite field. Along each of the boundaries between feldspathic arenite and litharenites and between feldspathic arenite and lithic arkose, 1 sample is plotted (Fig. 2a). Plots within the litharenite, feldspathic arkose and subarkose fields are associated with high amounts of quartz and therefore, the samples are characterized by slight mineralogical maturity. In the diagram used for geochemical classification of the sandstones by Pettijohn *et al.* (1987), 15 out of 16 samples fall in the litharenites field and only 1 in the subarkose field (Fig. 2b). This also indicates slight mineralogical maturity of the sandstones. Within the litharenites field, 2 samples show close affinity to arkose and 1 to subarkose. The small sample number (n=16) analyzed geochemically precludes sensible application of statistical or facies-based further analysis. The sandstone-types derived from the two classification schemes differ (Figs. 2a, b) as in the modal classification only the mineralogy of the framework grains of medium-grained sandstones are considered while in the chemical classification the whole rock chemistry of fine-grained sandstone is considered. In the latter case the chemical character of the protolith is more reflected probably because of the inclusion of matrix in the analyses. Each scheme thus has advantages and each is a standard method applied in sandstone provenance analysis, and both are thus used in this paper.

5. SEDIMENTARY FACIES

Sedimentary facies of the Middle Siwalik depositional sequence have been worked out in detail from the Tista valley section adjacent to the present area and have been presented in Kundu *et al.* (2011) and Kundu *et al.* (2012). Similar facies and associations are found in the Lish River section (Kundu, 2012). The Middle Siwalik here is a repeated sequence, stacked by five thrust faults (Fig. 1c) where the BT-3 thrust sheet carries the thickest part of the sequence, consisting of all types of facies occurring, in repetition. Therefore, the litholog (Fig. 3) has been constructed from the BT-3 sheet to represent the Middle Siwalik sequence in the Lish Valley. All other thrust sheets preserve the sequence partially and the thicknesses of the sequence in those sheets are less than that in the BT-3 sheet. The ~250m thick sequence is dominated by sandstone beds while conglomerate and siltstone-mudstone beds are subordinate members. Four distinct types of sandstone facies are identified: medium-grained sandstone (mostly arkosic) (S1); coarse- to medium-grained sandstone (litharenites and arkose) with pebbles (S2); coarse- to medium-grained sandstone (dominantly arkosic,

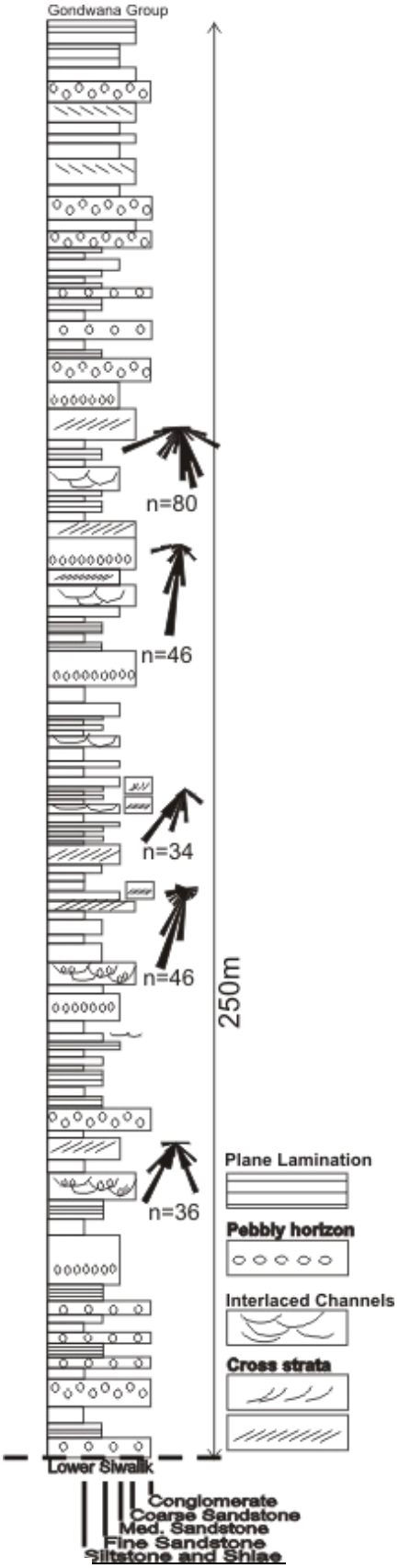

Figure 3. Stratigraphic column of the Middle Siwalik Subgroup in the Lish River section showing palaeocurrent pattern at different stratigraphic levels.

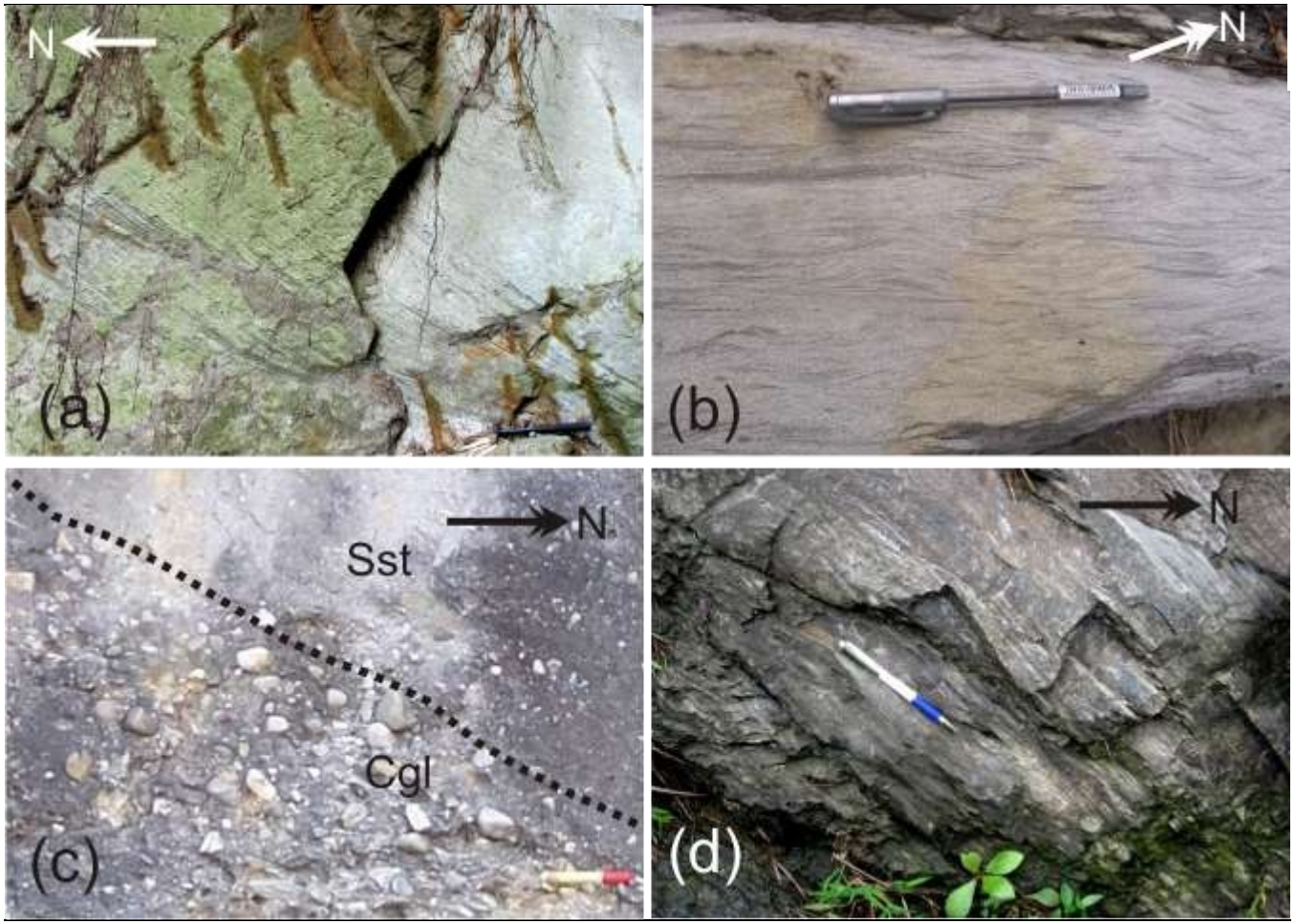

Figure 4. (a) Field photograph of megaripple cross-strata within a thick sandstone bed of S1 facies. The cross-strata are at low angle with the bedding plane (marked by broken line). Length of hammer 31cm.; (b) Field photograph of S4 facies unit consisting small-scale ripple bedding . Length of pen 15cm.; (c) Field photograph showing gradational contact (marked by dotted line) between matrix-supported conglomerate bed (Cgl) of the C2 facies and pebbly sandstone (Sst) of the S2 facies. Length of pen is 15cm; (d) Field photograph of a unit of M1 facies consisting siltstone-mudstone laminae. Length of pen 15cm.

some litharenites) without pebbles (S3); and fine grained sandstone (arkosic) (S4). Facies S1 consists of thick beds showing normal grading and preserves plane laminae, tabular cross-stratification, and megaripple cross-strata (Fig. 4a); S2 consists of trough cross-strata and channel structures, often interlaced, with pebbles at the channel bases; S3 comprises sheet-sand bodies without any other primary structure, and facies S4 is plane laminated and often with small-scale ripples (Fig. 4b). The conglomerate members of the sequence can be classified into four distinct facies: crude cross-stratified matrix-supported (matrix > framework) conglomerates facies (C1) where volume of matrix in the rocks is greater than that of framework clasts; beds of this facies show randomly arranged angular to subrounded pebbles; matrix-supported conglomerate (matrix > framework) in thick beds without any conspicuous primary structure (C2) (Fig. 4c); clast-supported cross-stratified conglomerate facies (framework > matrix) with pebble imbrication and crude planar cross-strata defined by arrangement of pebbles (C3); matrix-supported conglomerate beds with or without grading and with channel structures and trough cross-strata (C4). In the other two facies types, siltstone and mudstone are the dominant lithotypes. Composite bedsets of siltstone-mudstone, completely devoid of sandstone, with plane laminae form the M1 facies (Fig. 4d). In the heterolithic (interlayered package of thin sandstone, siltstone and mudstone beds) units (Facies H1) plane laminae, small scale ripple laminae and small scale cross-strata are common primary structures. The pre-thrusting palaeocurrent pattern shows maximum spread between SW and SE at almost all stratigraphic levels (Fig. 3). Minor spreads towards east and west are also evident at different stratigraphic levels (Fig. 3).

6. SANDSTONE PETROGRAPHY

In the studied sandstones the framework grains consist mainly of quartz, orthoclase, plagioclase and rock fragments. Grains of quartz (~65-55% of the volume of rock) are usually (~80-90% of the quartz grains) monocrystalline (Fig. 5a) with subordinate amounts of polycrystalline grains (Fig. 5b) having either straight or wavy grain margins. Quartz grains are angular to subrounded with either irregular or smooth grain boundaries. Most of the quartz grains (~65%) show sweeping undulose extinction (Fig. 5a). Grains of feldspar constitute ~15-20% of the volume of rock. Both alkali and plagioclase feldspars are present. Most of the feldspars are orthoclase (~90%). Feldspar grains are angular to subrounded and some alkali feldspars show perthite intergrowths (Fig. 5c). They are either unaltered or are partially altered to sericite (Fig. 5c). Undulose extinction is seen in many (~30%) of the feldspar grains. In some plagioclase feldspar grains the twin lamellae are kinked. Rock

Figure 5. (a) Photomicrograph of a sandstone sample showing monocrystalline quartz grain (Q), quartz shows undulose extinction (Qu). Carbonate (C) is present in intergranular spaces. Between crossed Nicols; (b) Photomicrograph of a sandstone sample with fragment of polycrystalline quartz (Q), mica schist (M) and cataclastic fragment (C). Between crossed Nicols; (c) Photomicrograph of a sandstone sample shows a feldspar grain with perthite intergrowth (Pe), partially sericitised orthoclase (P), and bent mica flake (M) showing undulose extinction. Between crossed Nicols.

fragments (constituting ~10% of the volume of rock) are represented by quartzite, chert, gneiss, slate, phyllite, mica schist and fragments of cataclasite showing clast-in-matrix texture (Fig. 5b). Biotite and muscovite flakes are bent or kinked and show undulose extinction (Fig. 5c).

Matrix constitutes ~5-10% of the volume of rock and is made up of silica and tiny biotite flakes. Silica cement is recrystallised. Carbonate is present along fractures and also in the intergranular spaces (Figs. 5a) which indicate precipitation of carbonate in the sandstones after deposition of the sediments.

7. MODAL ANALYSIS

Modal compositional data (percentage of grain-counts from the framework, Table 2) were plotted in ternary diagrams. In the Qm-F-Lt and Qt-F-L diagrams (Dickinson 1985; Dickinson *et al.* 1983) the plots fall in the 'recycled orogen' and 'quartzose recycled' fields, respectively (Figs. 6a, b). In the Qp-Lv-LS diagram (Dickinson and Suczek 1979) the plots are in the 'collisional orogen sources' field (Fig. 6c).

8. INTERPRETATION OF GEOCHEMICAL DATA

8.1. Major elements

The SiO_2 content in the rocks varies from ~55.5% to ~87.5% with an average of 72.6%, suggesting very high quartz content. CaO (~0.2% to ~2.5%) and Na_2O (~0.3% to ~2%) were possibly contributed by plagioclase whereas moderate K_2O (~1.5% to ~4.5%) content probably reflects contribution from K-feldspars and mica. The K_2O and Na_2O values support the petrographic observation that orthoclase dominates over plagioclase. High Al_2O_3 (~7% to ~21%) content suggests the presence of clay minerals and micas while low TiO_2 (0.25% to ~0.9%) content indicates rarity of Ti-bearing minerals.

The TiO_2-Al_2O_3 ratios suggest depletion of Ti-bearing minerals. The TiO_2 vs. Al_2O_3 plot (Fig. 7a) (cf. Amajor 1987) shows that the analysed samples fall in the granite and granite-basalt fields. In analyzing the major element geochemical data here, discriminant function analysis, which is a standard statistical method, is used. This analysis basically produces a set of linear functions which are derived from multiple variables (in this case various major element ratios) to enable the greatest separation between groups of standard data; the latter groups are pre-defined (e.g., Roser and Korsch 1988). In this paper the pre-defined groups are either different provenance terranes or different plate tectonic settings, and several detailed methods towards these two ends are applied. Application of discriminant function analysis to

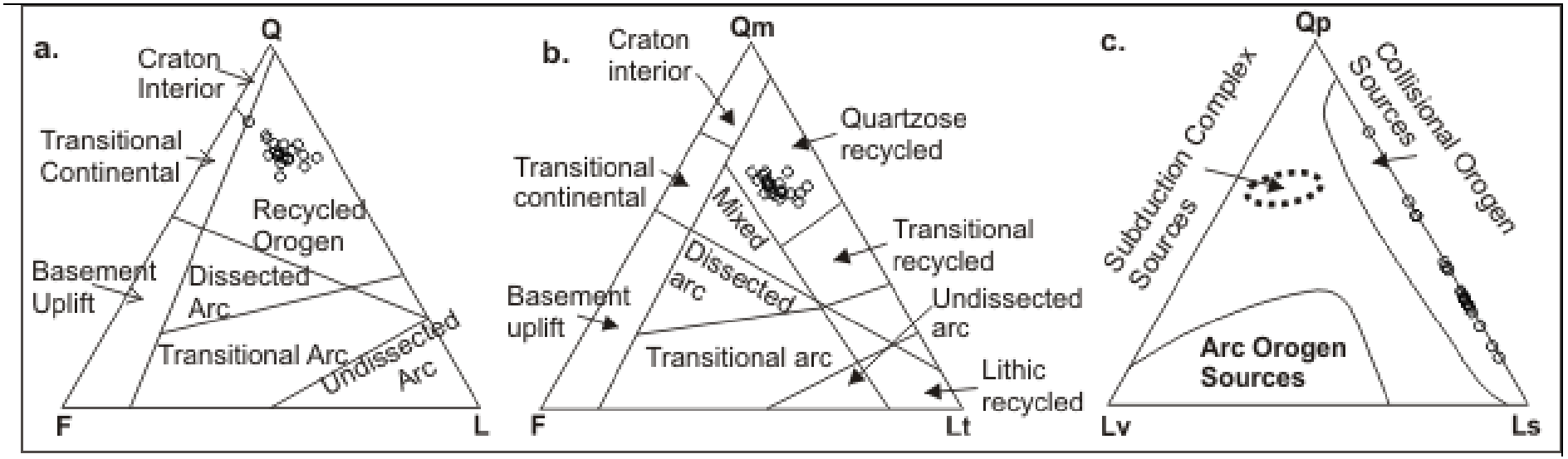

Figure 6. Ternary plots of modal values of framework components in Middle Siwalik sandstones on Lish valley. (A) Q-F-L plots in the recycled orogenic provenance field (cf. Dickinson 1985); (B) Qm-F-Lt plots in the quartzose recycled provenance field (cf. Dickinson *et al.* 1983); (C) Qp-Lv-Ls plots in the collisional orogen sources for the detritus (cf. Dickinson and Suczek 1979).

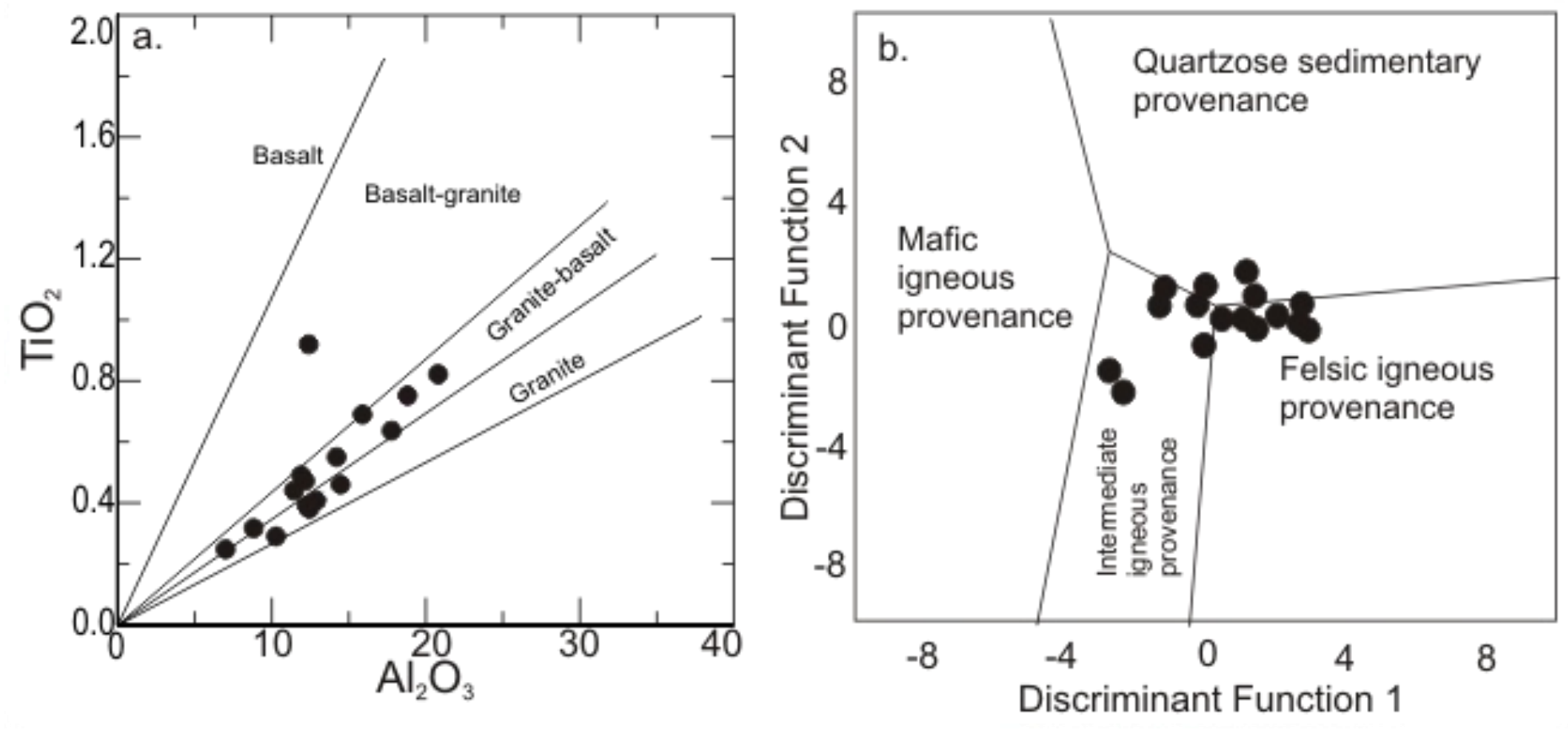

Figure 7. (a) Al_2O_3 vs. TiO_2 plot to decipher provenance lithology after Amajor (1987); (b) Discriminant function diagram (after Roser and Korsch 1988) reflecting intermediate to felsic character of provenance.

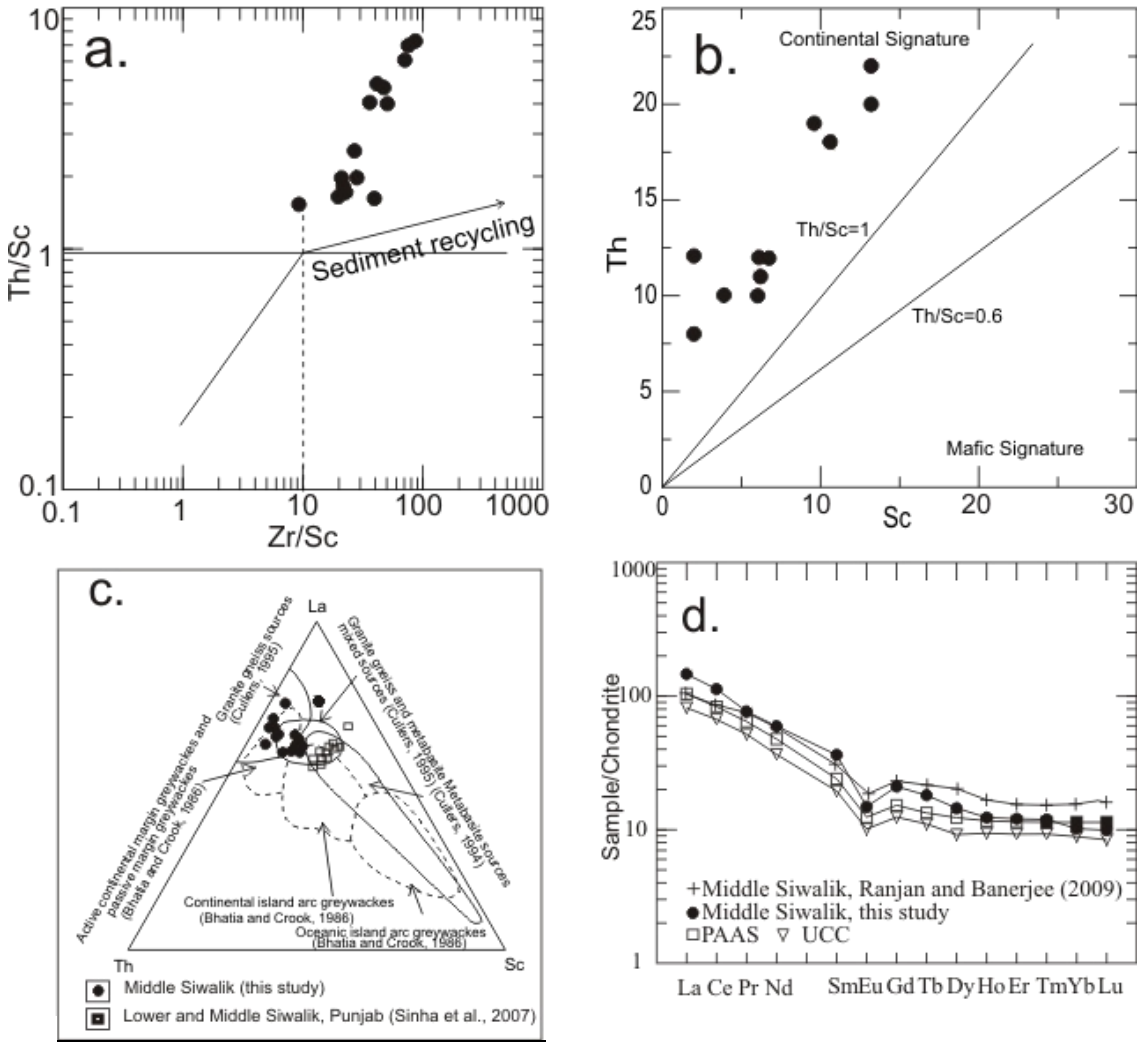

Figure 8. (a) Diagram (after Roser and Korsch 1986) for differentiation of plate tectonic settings. Note that Siwalik rocks of present area and from western Himalaya are plotted in the Passive Margin field; (b) Discriminant diagram (after Maynard *et al.* 1982) for differentiation of plate tectonic settings. PM-Passive margin, ACM-Active continental margin. Note that Siwalik rocks of present area and from western Himalaya are plotted in the Passive Margin field; (c) Discriminant function diagram (after Bhatia 1983) reflecting the tectonic settings of the provenance of Middle Siwalik sandstones; (d) Major element plots on the tectonic setting discrimination diagram after Kroonenberg (1994). A: Oceanic island Arc, B: continental island Arc, C: active continental margin, D: passive margin.

geochemical data for sandstones has shown an acceptable level of success, bearing in mind that sediment transport and concomitant grain size changes, diagenesis and weathering play a role in addition to source area compositions (e.g., Roser and Korsch 1986; 1988; Bhatia 1983; Bhatia and Crook 1986).

These discriminant functions involve ratios of TiO_2, Fe_2O_3, MgO, Na_2O and K_2O to Al_2O_3 and circumvent the problem of non-clastic calcium oxide and silica. The plots of discriminant function values for the analysed samples in the discriminant diagram (Fig. 7b) are spread in the intermediate igneous (6 data points), felsic igneous (7 points) and quartzose sedimentary provenance (3 points) fields. The few points that fall in the quartzose sedimentary field possibly indicate recycling of sediments initially derived from felsic/intermediate sources.

Roser and Korsch (1986) and Maynard *et al.* (1982) have used major element oxide discriminant function diagrams to unveil provenance settings. Discriminant functions using Al_2O_3, TiO_2, Fe_2O_3T, MgO, CaO, Na_2O, and K_2O in the discriminant diagram proposed by Bhatia (1983) enable characterisation of the tectonic setting of the provenance. Four source settings: ocean island arc, continental island arc, passive margin (PM) and active continental margin (ACM), are discriminated through this diagram. Kroonenberg (1994) used major element oxide values in a ternary plot also to discriminate between the provenance settings. In the Na_2O/K_2O vs. SiO_2 diagram (Fig. 8a) (cf. Roser and Korsch 1986) all the plots are in the passive margin (PM) field. Similar distribution is found in the SiO_2/Al_2O_3–K_2O/Na_2O plots (Fig. 8b) (cf. Maynard *et al.* 1982). In the discriminant diagram used by Bhatia (1983) (Fig. 8c) 12 samples plot in the PM field, 2 in the ACM field and 2 on the boundary between these two fields. In the $SiO_2/20$-K_2O+Na_2O-TiO_2+Fe_2O_3+MgO diagram (Fig. 8d) (cf. Kroonenberg 1994) also, the samples plot in the PM Field with only one exception which is plotted in the continental island arc field.

For siliciclastic rocks some other major oxide plots that can potentially be used (e.g. K_2O/Na_2O and $Al_2O_3/(CaO+Na_2O)$ vs. (Fe_2O_3+MgO); Bhatia 1983) often show widely scattered patterns of data points, mainly due to considerable carbonate in matrix, secondary alteration in feldspars and rock fragments, and also abundant detrital muscovite and insignificant amounts of feldspars (Mader and Neubauer 2004) and, therefore are excluded here as those plots are inappropriate for interpretations.

8.2. Trace and rare earth elements

McLennan (1989) has shown that changes during transport of sediment and diagenesis after deposition can affect the sedimentary geochemical record, which may lead to erroneous

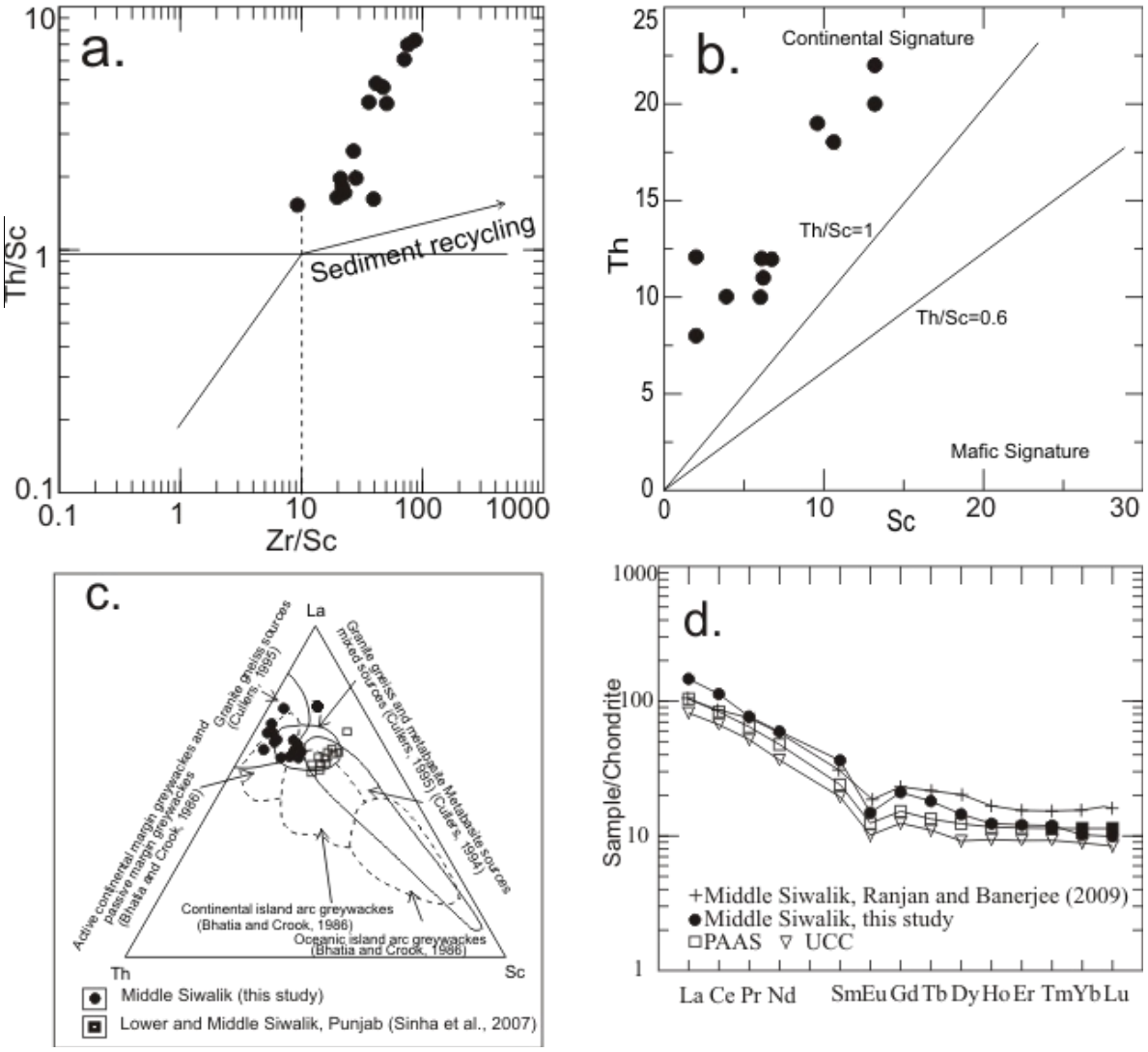

Figure 9. (a) Th/Sc vs. Zr/Sc plots (after McLennan *et al.* 1993) of Middle Siwalik sandstones reflecting increased concentration of heavy minerals by prolonged reworking; (b) Th vs Sc plots for comparison with linear provenance indicators (after Chakrabarty, 2009 and references therein; (c) Discrimination diagram for differentiation of tectonic setting and rock types (after Bhatia and Crook (1986) and Cullers (1995). Note that samples of present study and from Punjab recess (Sinha *et al.* 2007) show granite-gneiss and metabasic mixed provenance; (d) Diagram comparing chondrite-normalized REE pattern for Middle Siwalik foreland sediments with REE values of Upper Continental crust (UCC) and Post-Archaean Australian Shale (PAAS) values. Almost similar pattern is shown by Middle Siwalik samples from Kangra and DehraDun sub-basins (Ranjan and Banerjee 2009).

interpretation from geochemical data and particularly for the more mobile major element oxide data. Studies have also recommended that the amounts of some trace elements and REE, which are less mobile in comparison to the major elements reflect their concentrations in the sources and are therefore useful indicators of the process of sedimentation, provenance and tectonic setting (Cullers 1988; Bhatia and Crook 1986; Taylor and McLennan 1985; Cullers and Stone 1991; McLennan *et al.* 1993).

Trace element concentrations in sedimentary rocks help in revealing the composition of the extant crust, particularly the upper continental crust from which detritus was derived. The useful elements are Th, Ni, Y, Cr and REEs. In the Middle Siwalik samples the Cr/V (0.7 to 11.5) values are well below those typical for mafic sources, while high Y/Ni (0.6 to 5) and low Cr/V values indicate felsic source rocks (c.f. Hiscott 1984; Dinelli *et al.* 1999; de Luchi *et al.* 2002). According to Bhatia and Crook (1986) La/Th values are within 1.77-2.36 in the meta-sandstones of continental margins and reflect some basic detritus input if the value is greater than 3. La/Th values (~1.9 to ~3.6 with only two samples with the ratio above 3) of the analysed samples therefore, mostly indicate continental margin setting with some relatively minor basic input.

The Th/Sc ratio is an index of provenance. The ratio is higher in samples from active margin settings than from passive margins (McLennan *et al.* 1990). Hydraulic sorting and reworking during sedimentation lead to concentration of resistant phases like zircon. The Zr:Sc (9.3 to 88.5) ratios are more than 10 in all the Middle Siwalik samples except one, while the Th:Sc ratios (1.5 to 7.4) are more than 1 in all samples; taken together, these data indicate continental igneous sources with intense reworking of the sediment that has increased the concentration of Zr (de Luchi *et al.* 2002). A negative slope with a shift towards the higher values is shown by the plots in the Zr/Sc against Th/Sc diagram (Fig. 9a) (cf. McLennan *et al.* 1993) and a shift towards higher values of both parameters indicates increased concentration of heavy minerals which is possibly an indication of prolonged recycling of the sediments.

Plate-tectonic settings of palaeo-basins of sedimentation are generally discriminated from bivariate and trivariate plots of trace elements (Bhatia and Crook 1986; Cullers 1995). Middle Siwalik data points in the Th-Sc diagram are within the field of source with 'continental signature' (Fig. 9b) (c.f. Chakrabarty *et al.* 2009 and references therein). Plots in the La-Th-Sc ternary diagram are mainly in the granite-gneiss source field with subordinate metabasic input. In this diagram the data plots are also within the fields of PM and/or ACM settings (Fig. 9c) (cf. Bhatia and Crook 1986; Cullers 1995).

The chondrite normalized REE values match well with Post-Archaean Australian shale (PAAS) and Upper Continental Crustal (UCC) values (Fig. 9d) (cf. Taylor and McLennan 1985, 2001). An almost similar pattern is shown by Middle Siwalik samples from the Kangra and DehraDun sub-basins (Ranjan and Banerjee 2009). The steep LREE, almost flat HREE and negative Eu anomaly indicate a continental source (after Taylor and McLennan 1985; Gromet *et al.* 1984).

9. DEPOSITIONAL SETUP

In the ~250m thick Middle Siwalik sequence (Fig. 2) each facies is repeated and similar associations are also reported from the adjacent section of Siwalik rocks along the Tista River section (Kundu *et al.* 2012). The facies S1 bears characters of longitudinal bar deposits along the channel banks in the mid-fan region of alluvial fans (cf. Miall 1992; 1996; Mazumder 2002; Zielinski and van Loon 1999b). The S2 facies indicates deposition in a high-energy setting of proximal-fan as characterised by coarse sand, pebbles at channel bases (cf., Zielinski and van Loon 1999a; Zakir Hossain *et al.* 2002; Kundu *et al.* 2012) or in mad-fan setup with coalescing or interlacing channels (Opluštil *et al.* 2005). Sheet sand geometry without any channelised deposit and absence of any other primary structure in S3 facies units together point to waning energy flood deposits possibly in distal fans (e.g., Zavala 2008; MacCarthy 1990; Sadler and Kelly 1993). Thick conglomerate beds of the C1 facies, sparse presence of grading, planar stratification of the C1 units and absence of sedimentary structures in facies C2 indicate deposition in the proximal fan (cf., Miall 1996; Zielinski and van Loon 1999b; Neves *et al*. 2005). C3 and C4 facies indicate mid-fan deposition preserving signatures of bar migration and lateral channel-shifts in the braided region of alluvial fans (cf., Reineck and Singh, 1975; Miall 1977; Opluštil *et al.* 2005; Casshyap and Tewari, 1984). Fine-grained facies (S4, H1 and M1) indicate deposition from suspension load in low energy condition possibly within shallow braided channels in distal-fan settings (cf., Rust 1972; Kumar and Tandon 1985; Dreyer, 1993). The facies attributes and the palaeocurrent data together led us to conclude that the Middle Siwalik sediments in the area were deposited in a major alluvial fan with a SW trending fan-axis. The major orogen-transverse channel system was possibly flowing towards the SSW through the fan. The alluvial system therefore, has most probably brought the sediment load from the Lesser and Higher Himalaya to the north. Palaeocurrent data indicate that a major alluvial and several smaller (higher order) alluvial fans formed by tributaries of the first order stream together formed a coalescing alluvial fan. Repetition of the similar facies and also the palaeocurrent patterns together also point to

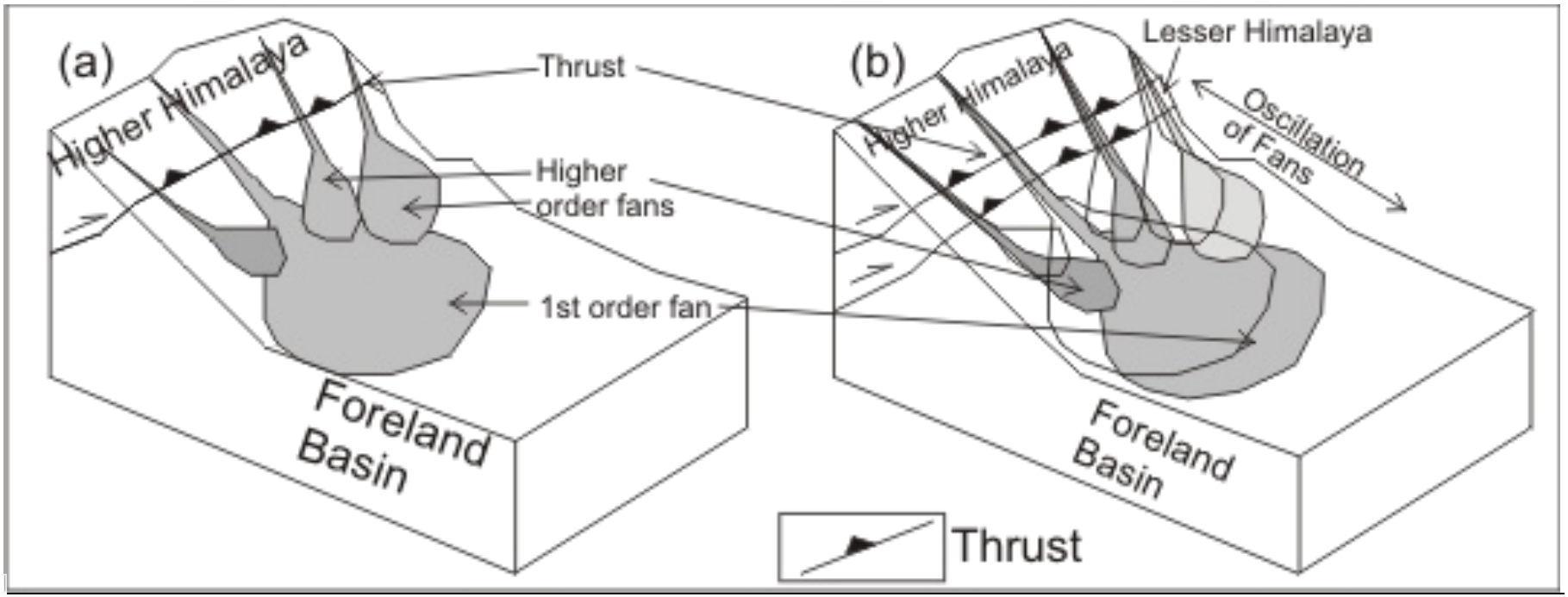

Figure 10. Scematic diagrams showing (a) formation of a coalescing alluvial fan at the foothils of the Himalaya before propagataion of the Lesser Himalayan Thrusts and (b) oscillation of the fan system in time and space with forelandward propagation of the lesser himalayan thrusts.

shifting of the major as well as minor fans with time resulting in deposition in different sub-basins of the alluvial fan system, partly one above the other. Repetitive basin-ward progression of thrust fronts pushing the mountain front towards the then foreland basin and intermediate erosional phases could also have caused such facies repetitions (cf. Raiverman 2002; Kundu *et al.* 2012) (Fig. 10).

10. DISCUSSION

In the Eastern Himalaya the Higher Himalayan lithologies consist of Precambrian granitic-gneissic rocks (Paro-Lingtse Gneiss and Darjeeling Gneiss) and the Lesser Himalayan succession consists of phyllites, chlorite-schists and metabasic slates (Table 1; Acharyya 1994; Matin and Mukul 2010). Analysis of facies attributes of the Middle Siwalik sedimentary rocks and palaeocurrent data reveals deposition in a coalescing alluvial fan depositional setup where the sub-environments were shifted with time due to repetitive propagations of thrust faults and intermediate erosional regimes. The first-order stream was a SSW directed one that brought sediment load from the elevated hinterland to debouch into the Middle Siwalik basin.

Sandstone provenance is analysed through sandstone grain mineralogy of medium-grained sandstones, and by whole rock geochemistry of fine-grained sandstones. The first method allows discrimination of detrital and diagenetic components and also enables study of grain textures; these advantages of the mineralogical method are balanced by the geochemical method being much faster and lacking point-counting errors (Rollinson 1993; Von Eynatten *et al.* 2003). Mineralogy and geochemistry of the studied sandstone samples of the Middle Siwalik sequence show that the sediments were derived chiefly from felsic to intermediate plutonic and low grade metamorphic sources. Therefore, the Precambrian gneisses namely the Paro-Lingtse Gneiss and Darjeeling Gneiss of the Higher Himalaya and the metabasic rocks of the Lesser Himalaya can be logically considered as the main source rocks. All of these three rock groups are older than the India-Tibet collision event that occurred ~55My ago (Yin and Harrison 2000). The presence of both monocrystalline and polycrystalline quartz, quartz and feldspar grains with different degrees of roundness, quartz and feldspar grains with different intensities of undulose extinction, feldspar grains with various degrees of alteration, presence of deformed and undeformed mica flakes and presence of different types of lithic fragments in the framework of the sampled sandstones indicate mixing of materials from spatially separated source rocks. Cataclasite fragments indicate presence of fault-rocks in the source area. Fragments of various rocks (quartzite, chert, phyllite, mica

schist and gneiss) suggest derivation of sediment from fold-and-thrust belts (Dickinson and Suczek 1979; Franzinelli and Potter 1983; Dickinson 1985). Modal values of framework components also suggest that the sediments were derived from an orogenic source. Major element oxide plots (TiO_2 – Al_2O_3), major element discriminant plots and trace element ratios (Th/Sc, La/Th, Y/Ni and Cr/V) suggest mixing of detritus dominantly from felsic source with subordinate input from mafic source in a continental setting. REE values also suggest a continental source of the Middle Siwalik sediments. Trace element values show enrichment of resistant minerals like zircon and the Th/Sc vs Zr/Sc plot suggests prolonged recycling of sediments which is possible in an orogenic setup. The inferred passive margin and subordinate active continental margin setting of the source rocks as reflected from various plots of major element-oxides and trace elements, therefore point to the rocks of a pre-collision continental margin.

Major and trace element plots used for understanding the character and possible tectonic setting of provenance lithologies and the recycling history related to Middle Siwalik sedimentation in the area of study are compared with Siwalik sediments of the western Himalaya presented by Sinha *et al.* (2007) and Ranjan and Banerjee (2009). The comparisons show similarly interpreted tectonic settings. Observed differences in rock types and recycling history are possibly due to inclusion of the Lower and Upper Siwalik rocks in the works of Sinha *et al.* (2007) and Ranjan and Banerjee (2009) whereas this study deals only with the Middle Siwalik succession. After the Himalayan collision the Darjeeling Gneiss and Paro-Lingtse Gneiss were thrust upward due to the activation of the Main Central Thrust (MCT) system (Yin 2006; Bhattacharyya and Mitra 2009) followed by the uplift of the Daling Group by the Ramgarh Thrust (Bhattacharyya and Mitra 2009). Meigs et al. (1995) suggested a Middle to Late Miocene age for the MBT, the thrust which has transported the Lesser Himalayan rocks over the Siwalik sediments. It can thus be envisaged that the uplift of the Lesser Himalaya in this region was concomitant with the Late Miocene Middle Siwalik sedimentation.

ACKNOWLEDGEMENTS

Abhik Kundu acknowledges the UGC, India, for the research grant PSW-035/10-11(ERO), and PGE thanks the University of Pretoria and National Research Foundation of South Africa for funding. The authors acknowledge Dr. P. P. Khanna, Wadia Institute of Himalayan Geology for chemical analysis of the samples. Helps extended by Dr. Dipak Kumar Kar, Dr. Biswajit Ghosh, Reetom Chaudhuri and Debaditya Bandyopadhyay are also appreciated.

REFERENCES

Acharyya, S.K. 1994. The Cenozoic Foreland Basin and tectonics of the eastern sub-Himalaya: problems and prospects. In: *Siwalik Foreland Basin of Himalaya,* Kumar, R., Ghosh, S.K., Phadtare, N.R. (eds). Himalayan Geology **15**, 3-21.

Acharyya, S.K., Shastry, M.V.A. 1979. Stratigraphy of the Eastern Himalaya. Himalayan Geology Seminar, New Delhi, *Geological Survey of India, Miscellaneous Publication* **41**, 49-64.

Aitchison, J. 1986. The Statistical Analysis of Compositional Data. Chapman and Hall, London.

Amajor, L.C. 1987. Major and trace element geochemistry of Albian and Turonian shales from the Southern Benue trough, Nigeria. *Journal of African Earth Sciences* **6**, 633-641.

Armstrong-Altrin, J.S., Verma, S.P, Madhavaraju, J., Ramaswami, S. 2004. Geochemistry of sandstones from the Upper Miocene Kudankulam Formation, Southern India: Implications for provenance, weathering and tectonic setting. *Journal of Sedimentary Research* **74(2)**, 285-297.

Asiedu, D.K., Suzuki, S., Shibata, T. 2000. Geochemistry of Lower Cretaceous sediments, inner zone of southwest Japan: constraints on provenance and tectonic environment. *Geochemical Journal* **34**, 155-173.

Banerji, I., Banerji, S. 1982. A coalescing alluvial fan model of the Siwalik sedimentation -a case study in the eastern Himalaya. *Geological Survey of India Miscellaneous Publication* **41**, 1-12.

Basu, A. 2003. A perspective on quantitative provenance analysis. In: *Quantitative Provenance Studies in Italy,* Valloni, R., Basu, A. (eds). Memorie Descrittive della Carta Geologica dell'Italia **61**, 11-22.

Bhatia, M.R. 1983. Plate tectonics and geochemical composition of sandstones. *Journal of Geology* **91**, 611-627.

Bhatia, M.R. 1985. Rare earth element geochemistry of Australian Paleozoic graywackes and mudrocks: Provenance and tectonic controls. *Sedimentary Geology* **45**, 97-113.

Bhatia, M.R., Crook, K.A.W. 1986. Trace element characteristics of greywackes and tectonic setting discrimination of sedimentary basins. *Contributions to Mineralogy and Petrology* **92**, 181-193.

Bhattacharyya, K. Mitra, G. 2009. A new kinematic evolutionary model for the growth of a duplex-an example from the Rangit duplex, Sikkim Himalaya, India. *Gondwana Research* **16**, 697-715.

Blatt, H., Middleton, G., Murray, R. 1980. Origin of Sedimentary Rocks. Prentice-Hall, Englewood Cliffs, New Jersey.

Blenkinsop, T. **2002.** *Deformation Microstructures and Mechanismsin in Minerals and Rocks*. 150 pp. Kluwer Academic Publishers, Netherlands.

Caracciolo, L., Von Eynatten, H., Tolosana-Delgado, R., Critelli, S., Manetti, P., Marchev, P. 2012. Petrological, geochemical, and statistical analysis of Eocene–Oligocene sandstones of the Western Thrace Basin, Greece and Bulgaria. *Journal of Sedimentary Research* **82 (7)**, 482-498.

Casshyap, S.M., Tewari, R.C. 1984. Fluvial models of the Lower Permian coal measures of Son-Mahanadi and Koel-Damodar Valley basins, India. *International Association of Sedimentologists, Special Publication* **7**, 121-147.

Chakrabarti, G, Shome, D, Bauluz, B., Sinha, S. 2009. Provenance and Weathering History of Mesoproterozoic Clastic Sedimentary Rocks from the Basal Gulcheru Formation, Cuddapah Basin, *Journal Geological Society of India **74***, 119-130.

Chaudhri, R.S. 1971. Petrogenesis of Cenozoic sediments of north-western Himalayas. *Geological Magazine* **108**, 43-48.

Compton, R.R. 1985. *Geology in the Field*, 1st Edition. 398pp. Wiley, New York.

Condie, K.C. 1991. Another look at rare earth elements in shales. *Geochimica et Cosmochimica Acta* **55**, 2527-2531.

Critelli, S., Garzanti, E., 1994. Provenance of the Lower Tertiary Murree redbeds (Hazara-Kashmir Syntaxis, Pakistan) and initial rising of the Himalayas. *Sedimentary Geology* **89**, 265-284.

Critelli, S., Ingersoll, R.V. 1994. Sandstone petrology and provenance of the Siwalik Group (northwestern Pakistan and western-southeastern Nepal). *Journal of Sedimentary Research* **A64(4)**, 815-823.

Critelli, S., De Rosa, R., Platt, J.P. 1990, Sandstone detrital modes in the Makran accretionary wedge, southwest Pakistan: Implications for tectonic setting and long-distance turbidite transportation. *Sedimentary Geology* **68**, 241-260.

Critelli S., Mongelli G., Perri F., Martin-Algarra A., Martin-Martin M., Perrone V., Dominici R., Sonnino M., Zaghloul M.N. 2008, Sedimentary Evolution of the Middle Triassic -Lower Jurassic continental redbeds from Western-Central Mediterranean Alpine

Chains based on geochemical, mineralogical and petrographical tools. *Journal of Geology*, **116**, 375-386.

Crook, K.A.W. 1974. Lithogenesis and geotectonics: the significance of compositional variation in flysch arenites (graywackes). In: *Modern and Ancient Geosynclinal Sedimentation,* Dott Jr., R.H., Shaver, R.H. (eds). SEPM Special Publication **19**, 304-310.

Cullers, R.L. 1988. Mineralogical and chemical changes of soil and stream sediments formed by intense weathering of the Danberg granite, Georgia, USA. *Lithos 21*, 301-314.

Cullers, R.L. 1994. The controls on the major and trace element variation of shales, siltstones and sandstones of Pennsylvanian-Permian age from uplifted blocks in Colorado to platform sediment in Kansas, USA. *Geochimica et Cosmochimica Acta* **22**, 49554972.

Cullers, R.L. 1995. The controls on major and trace element evolution of shales, siltstones, and sandstones of Ordovician to Tertiary age in the Wet Mountains region, Colorado, USA. *Chemical Geology* **123**, 107-131.

Cullers, R.L., Stone, J. 1991. Chemical and mineralogical composition of the Pennsylvanian mountain, Colorado, USA (an uplifted continental blocks) to sedimentary rocks from other tectonics environments. *Lithos* **27**, 115-131.

de Luchi, López, M.G., Hoffmann, A., Siegesmund, S., Wemmer, K., Steenken, A. 2002. Temporal constraints on the polyphase evolution of the Sierra de San Luis. Preliminary report based on biotite and muscovite cooling ages. In: Cabaleri, N., Linares, E., López de Luchi, M.G., Ostera, H., Panarello, H. (eds). Actas 15° Congreso Geológico Argentino (Proceedings of 15th Argentine Geological Congress) **1**, 309-315.

Decelles, P.G., Gehrels, G.E., Quade, J., Ojha, T.P., Kapp, P.A., Upreti, B.N. 1998. Neogene foreland basin deposits, erosional unroofing, and the kinematic history of the Himalayan fold-thrust belt, western Nepal. *Geological Society of America Bulletin* **110(1)**, 2-21.

Dickinson, W.R. 1970. Interpreting detrital modes of greywacke and arkose. *Journal of Sedimentary Petrology* **40**, 695-707.

Dickinson, W.R. 1985. Interpreting provenance relations from detrital modes of sandstones. In: *Provenance of Arenites*, Zuffa, G. G. (ed.). Reidel Publishing Co: Dordrecht, Netherlands; 333-361.

Dickinson, W.R. 1988. Provenance and sediment dispersal in relation to paleotectonics and paleogeography of sedimentary basins. In: *New Perspectives in Basin Analysis,* Kleinspehn, K.L., Paola, C. (eds). Springer-Verlag: New York; 3-25.

Dickinson, W.R., Beard, S.L., Brakenridge, R.G., Erjavec, J.L., Ferguson, R.C., Inman, K.F., Knepp, R.A., Lindberg, F.A., Ryherg, P.T. 1983. Provenance of North American Phanerozoic sandstones in relation to tectonic setting. *Geological Society of America Bulletin* **94**, 222-235.

Dickinson, W.R., Suczek, C.A. 1979. Plate tectonics and sandstone compositions. *American Association of Petroleum Geologists Bulletin* **63**, 2164-2182.

Dinelli, E., Testa, G., Cortecci, G., Barbieri, M. 1999. Stratigraphic and petrographic constraints to trace element and isotope geochemistry of Messinian sulfates of Tuscany. *Memorie della Societa Geologica Italiana (Memoir of the Italian Geological Society)* **54**, 61-74.

Dorsey, R.J. 1988. Provenance evolution and unroofing history of a modern arc-continent collision: Evidence from petrography of Plio-Pleistocene sandstones, eastern Taiwan. *Journal of Sedimentary Petrology* **58**, 208-218.

Folk, R.L. **1974.** *The petrology of sedimentary rocks.* Hemphill Publishing Co.: Austin, Texas.

Franzinelli, E., Porter, P.E. 1983. Petrology, chemistry and texture of modern river sands, Amazon river system. *Journal of Geology* **91**, 23-39.

Gansser, A.1964. *Geology of the Himalayas.* Wiley: New York.

Garzanti, E., Critelli, S., Ingersoll, R.V. 1996. Paleogeographic and paleotectonic evolution of the Himalayan Range as reflected by detrital modes of Tertiary sandstones and modern sands (Indus transect, India and Pakistan). Geological Society of America Bulletin, v. 108, p. 631-642.

Garzanti, E., Vezzoli, G. 2003. A classification of metamorphic grains in sands based on their composition and grade. *Journal of Sedimentary Research* **73**, 830-837.

Gazzi, P. 1966. "Le Arenarie del Flysch Sopracretaceo dell'Appennino Modenese: Correlazioni con il Flysch di Monghidoro". *Mineralogica et Petrografica Acta* **12**, 69-97.

Gromet, L.P., Dymek, R.F., Haskin, L.A., Korotev, R.L. 1984. The North American shale composite: its compilation and major and trace element characteristics. *Geochimica et Cosmochimica Acta* **48**, 2469-2482.

Hiscott, R. 1984. Ophiolitic source rocks for Taconic-age flysch: trace element evidence. *Geological Society of America Bulletin* **95**, 1261-1267.

Hodges, K.V. 2000. Tectonics of the Himalaya and southern Tibet from two perspectives. *Geological Society of America Bulletin* **112**, 324-350.

Holocombe, R.J. **1994**. GEOrient - an integrated structural plotting package for MS-Windows. *Geological Society Australia Abstracts*, **36**, 73-74.

Ibbeken, H., Schleyer, R. 1991. Source and Sediment. Springer, Berlin.

Ingersoll, R.V., Bullard, T.F., Ford, R.L., Grimm, J.P., Pickle, J.D., Sares, S.W. 1984. The effect of grain size on detrital modes: A test of the Gazzi-Dickinson point counting method. *Journal of Sedimentary Petrology* **54**, 103-106.

Khanna, P.P., Saini, N.K., Mukherjee, P.K., Purohit, K.K. 2009. An appraisal of ICP-MS technique for determination of REEs: long term QC assessment of Silicate Rock Analysis. *Himalayan Geology* **30(1)**, 95-99.

Kroonenberg, S.B. 1994. Effects of provenance, sorting and weathering on the geochemistry of fluvial sands from different tectonic and climatic environments. *Proceedings of the 29th International Geological Congress, Part A, Kyoto, Japan,* 69-81.

Kumar, R., Tandon, S.K. 1985. Sedimentology of Plio-Pleistocene late orogenic deposits associated with intra-plate subduction- The Upper Siwalik Sub-group of a part of Punjab sub- Himalaya, India. *Sedimentary Geology* **42**, 105-158.

Kundu, A., Matin, A., Mukul, M. 2012. Depositional environment and provenance of Middle Siwalik sediments in Tista valley, Darjiling District, Eastern Himalaya, India. *Journal of Earth System Science* **121(1)**, 73-89.

Kundu, A., Matin, A., Mukul, M., Eriksson, P.G. 2011. Sedimentary facies and soft-sediment deformation structures in the Late Miocene-Pliocene Middle Siwalik Subgroup, eastern Hi*malaya,* Darjiling district, India. *Journal of the Geological Society of India* **78**, 321-336.

Lee, Y.I., Sheen, D.H. 1998. Detrital modes of the Pyeongan Supergroup (Late Carboniferous-Early Triassic) sandstones in Samcheog coalfield, Korea: implications for provenance and tectonic setting. *Sedimentary Geology* **119(3-4)**, 219-238.

MacCarthy, I.A.J. 1990. Alluvial sedimentation patterns in the Munster Basin, Ireland. *Sedimentology* **37**, 685-712.

Mader, D., Neubauer, F. 2004. Provenance of Paleozoic sandstones from the Carnic Alps (Austria): petrographic and geochemical indicators. *International Journal of Earth Sciences* **93(2)**, 262-281

Malik, J.N., Nakata, T. 2003. Active faults and related Late Quaternary de formation along the northwestern Himalayan frontal zone, India. *Annals of Geophysics **46(5)***, 917-936.

Matin, A., Mukul, M. 2010. Phases of deformation from cross-cutting structural relationships in external thrust sheets: insights from small-scale structures in the Ramgarh Thrust sheet, Darjiling Himalaya, West Bengal. *Current Science* **99**, 1369-1377.

Maynard, J.B., Valloni, R., Yu, H.S. 1982. Composition of modern deep sea sands from arc related basins. *Geological Society of London Special Publication* **10**, 551-561.

Mazumder, R. 2002. Sedimentation history of the Dhanjori and Chaibasa formations, eastern India and its implications. Unpublished Ph.D. Thesis, Jadavpur University: Kolkata, India, 119p.

Mclennan, S.M. 1989. Rare earth elements in sedimentary rocks: influence of provenance and sedimentary processes. *Reviews in Mineralogy* **21**, 169-200.

Mclennan, S.M. Hemming, S., Mcdaniel, D.K., Hanson, G.N. 1993. Processes Controlling the Composition of Clastic Sediments. In: *Geochemical approaches to sedimentation, provenance, and tectonics*, Johnson, M.J., Basu, A. (eds). Geological Society of America, Special Paper **284**, 21–40.

Mclennan, S.M., Taylor, S.R., Mcculloch, M.T., Maynard, J.B. 1990. Geochemical and Nd-Sr isotopic composition of deep-sea turbidites: Crustal evolution and plate tectonic associations. *Geochimica et Cosmochimica Acta* **54**, 2015-2050.

Mclennan, S.M. 2001. Relationships between the trace element composition of sedimentary rocks and upper continental crust. *Geochemistry. Geophysics. Geosystems* **2**, 1021, doi:10.1029/2000GC000109.

Meigs, A.J., Burbank, D.W., Beck, R.A. 1995. Middle–late Miocene (>10 Ma) formation of the Main Boundary thrust in the western Himalaya. *Geology* **23(5)**, 423-426.

Miall, A. D. 1977. A review of the braided-river depositional environment. *Earth-Science Reviews* **13**, 1-62.

Miall, A.D. 1992. Alluvial deposits. In: *Facies Models: Response to Sea Level Change*, Walker, R.G., James, N.P. (eds). Geological Association of Canada, Waterloo, Ontario, 119–142.

Miall, A.D. 1996. *The Geology of Fluvial Deposits: Sedimentary Facies, Basin Analysis, and Petroleum Geology*. Springer-Verlag: Berlin.

Mukul, M. 2000. The geometry and kinematics of the Main Boundary Thrust and related neotectonics in the Darjiling Himalayan fold-and-thrust belt, West Bengal, India. *Journal of Structural Geology* **22**, 1261–1283.

Mukul, M. 2010. First-order kinematics of wedge-scale active Himalayan deformation: Insights from Darjiling-Sikkim-Tibet (DaSiT) wedge. *Journal of Asian Earth Sciences* **39**, 645-657.

Najman, Y., Garzanti, E. 2000. Reconstructing early Himalayan tectonic evolution and paleogeography from Tertiary foreland basin sedimentary rocks, northern India. *Geological Society of America Bulletin* **112**, 435-449.

Nesbitt, H. W., Young, G.M. 1989. Formation and diagenesis of weathering profile. *Journal of Geology* **97**, 129-147.

Neves, M. A., Morales, N., Saad, A.R. 2005. Facies analysis of tertiary alluvial fan deposits in the Jundiaí region, São Paulo, southeastern Brazil. *Journal of South American Earth Sciences* **19**, 513-524.

Opluštil, S., Martínek, K., Tasáryová, Z. 2005. Facies and architectural analysis of fluvial deposits of the Nýřany Member and the Týnec Formation (Westphalian D -Barruelian) in the Kladno-Rakovník and Pilsen basins. *Bulletin of Geosciences* **80(1)**, 45-66.

Parkash, B., Sharma, R.P., Roy, A.K. 1980. The Siwalik Group (molasses)-sediments shed by collision of continental plates. *Sedimentary Geology* **25**, 127-159.

Perri F., Critelli S., Martin-Algarra A., Martin-Martin M., Perrone V., Mongelli G. & Zattin M. 2013. Triassic redbeds in the Malaguide Complex (Betic Cordillera – Spain): petrography, geochemistry and geodynamic implications. *Earth Science Reviews* **117**, 1-28.

Pettijohn, F.J. 1975. *Sedimentary Rocks* (3rd edn.). Harper & Row: New York.

Pettijohn, F.J., Potter, P.E., Siever, R. 1987. *Sand and Sandstones* (2nd edn.). Springer-Verlag: New York.

Potter, P.E. 1986. South America and a few grains of sand, Pt. I. Beach sands. *The Journal of Geology* **94(3)**, 301-319.

Raiverman, V. 2002. *Foreland sedimentation in Himalayan tectonic regime: A Relook at the orogenic process*. Bishen Singh Mahendra Pal Singh: Dehradun, India.

Ragan, D.L. 2009. *Structural Geology: An Introduction to geometrical Techniques* (4th edn.). Cambridge University Press: New York.

Ranjan, N., Banerjee, D.M. 2009. Central Himalayan crystallines as the primary source for the sandstone-shale suites of the Siwalik Group: New geochemical evidence. *Gondwana Research* **16**, 687-696.

Reading, H.G., Levell, B.K. 1996. Controls on the sedimentary record. In: *Sedimentary ennvironments: processes, facies and stratigraphy*, Reading, H.G. (ed). Blackwell Science, Oxford, 5-36.

Reineck, H.-E. and Singh, I.B. 1975. Depositional sedimentary environments. Springer-Verlag: Berlin.

Rollinson, H.R. 1993. *Using Geochemical Data: Evaluation, Presentation, Interpretation.* Longman: Edinburg Gate, United Kingdom.

Roser, B.P., Korsch, R.J. 1986. Determination of tectonic setting of sandstone-mudstone suites using SiO2 content and K2O Na2O ratio. *Journal of Geology* **9**, 635-650.

Roser, B.P., Korsch, R.J./ 1988. Provenance signatures of sandstone-mudstone suites determined using discriminant function analysis of major-element data. *Chemical Geology* **67**, 119-139.

Rust, B.R. 1972. Structure and process in a braided river. *Sedimentology* **18**, 221-246.

Sadler, S.P., Kelly, S.B. 1993. Fluvial processes and cyclicity in terminal fan deposits: an example from the Late Devonian of southwest Ireland. *Sedimentary Geology* **85**, 375-386.

Schwab, F.L. 1975. Framework mineralogy and chemical composition of continental margin-type sandstones. *Geology* **3**, 487-490.

Schwan, W. 1980. Shortening structures in eastern and northwestern Himalayan rocks. In: *Current trends in Geology*, Saklani, P. S. (ed.). Today & Tomorrow Publishers: New Delhi; **series-3**, 1-62.

Selley, R. 1985. *Ancient Sedimentary Environments: And Their Sub-Surface Diagnosis* (3rd edn.). Cornell University Press: Ithaca, New York.

Sibson, R.H. 1977. Fault rocks and fault mechanisms. *Journal of the Geological Society* **133(3)**, 191-213.

Sinha Roy, S. 1967. Tectonic evolution of the Darjiling Himalayas. *Quarterly Journal of the Geological, Mining and Metallurgical Society of India* **48**, 167-178.

Sinha, S., Islam, R., Ghosh, S.K., Kumar, R., Sangode, J. 2007. Geochemistry of Neogene Siwalik mudstones along Punjab re-entrant, India: implications for source-area weathering, provenance and tectonic setting. *Current Science* **92**, 1103-1113.

Taylor, S.R., Mclennan, S.M. 1985. *The Continental Crust: Its Composition and Evolution*. Blackwell: Oxford, United Kingdom.

Valdiya, K.S. 1980. *Geology of the Kumaon Lesser Himalaya.* Wadia Institute of Himalayan Geology: Dehra Dun, India.

Von Eynatten, H., Barceló-Vidal, C., Pawlowsky-Glahn, V. 2003. Composition and discrimination of sandstones: a statistical evaluation of different analytical methods. *Journal of Sedimentary Research* **73/1**, 47-57.

Weltje, G.J. 2002. Quantitative analysis of detrital modes: statistically rigorous confidence regions in ternary diagrams and their use in sedimentary petrology. *Earth-Science Reviews* **57**, 211-253.

Weltje, G.J., Von Eyenatten, H. 2004. Quantitative provenance analysis of sediments: review and outlook. *Sedimentary Geology* **171,** 1-11

Yin, A. 2006. Cenozoic tectonic evolution of the Himalayan orogen as constrained by along-strike variation of structural geometry, exhumation history, and foreland sedimentation. *Earth-Science Review* **76**, 1-131.

Yin, A., Harrison, T.M. 2000. Geologic evolution of the Himalayan-Tibetan orogen. *Annual Review of Earth and Planetary Science* **28**, 211-280.

Zakir Hossain, H. M., Sultan-Ul-Islam, M., Ahmed, S. S., Hossain, I. 2002. Analysis of sedimentary facies and depositional environments of the Permian Gondwana sequence in borehole GDH-45, Khalaspir Basin, Bangladesh. *Geoscience Journal*, **6(3)**, 227–236.

Zavala, C. 2008. Towards a genetic facies tract for the analysis of hyperpycnal deposits. American Association of Petroleum Geologists, Hedberg Conference, March 3-7, Ushuaia-Patagonia, Argentina, Abstracts, 50-51,

Zielinski, T., van Loon, A. J. 1999a. Subaerial terminoglacial fans I: a semi-quantitative sedimentological analysis of the proximal environment. *Geologie en Mijnbouw (Netherlands Journal of Geosciences)* **77**, 1-15.

Zielinski, T., van Loon, A. J. 1999b. Subaerial terminoglacial fans II: a semi-quantitative sedimentological analysis of the middle and distal environments. *Geologie en Mijnbouw (Netherlands Journal of Geosciences)* **78**, 73-85.